Journal of Animal Ecology 2007
76, 424–438

Regional climate modulates the canopy mosaic of favourable and risky microclimates for insects

SYLVAIN PINCEBOURDE, HERVE SINOQUET*, DIDIER COMBES† and JEROME CASAS

*Institut de Recherche sur la Biologie de l'Insecte (IRBI, CNRS UMR 6035), Université François Rabelais, Faculté des Sciences et Techniques, 37200 Tours, France; *UMR PIAF INRA-Université Blaise Pascal, Site de Crouelle, 234 avenue du Brézet, 63100 Clermont-Ferrand, France; and †INRA Unité d'Ecophysiologie des Plantes Fourragères, 86600 Lusignan, France*

Summary

1. One major gap in our ability to predict the impacts of climate change is a quantitative analysis of temperatures experienced by organisms under natural conditions. We developed a framework to describe and quantify the impacts of local climate on the mosaic of microclimates and physiological states of insects within tree canopies. This approach was applied to a leaf mining moth feeding on apple leaf tissues.

2. Canopy geometry was explicitly considered by mapping the 3D position and orientation of more than 26 000 leaves in an apple tree. Four published models for canopy radiation interception, energy budget of leaves and mines, body temperature and developmental rate of the leaf miner were integrated. Model predictions were compared with actual microclimate temperatures. The biophysical model accurately predicted temperature within mines at different positions within the tree crown.

3. Field temperature measurements indicated that leaf and mine temperature patterns differ according to the regional climatic conditions (cloudy or sunny) and depending on their location within the canopy. Mines in the sun can be warmer than those in the shade by several degrees and the heterogeneity of mine temperature was incremented by 120%, compared with that of leaf temperature.

4. The integrated model was used to explore the impact of both warm and exceptionally hot climatic conditions recorded during a heat wave on the microclimate heterogeneity at canopy scale. During warm conditions, larvae in sunlight-exposed mines experienced nearly optimal growth conditions compared with those within shaded mines. The developmental rate was increased by almost 50% in the sunny microhabitat compared with the shaded location. Larvae, however, experienced optimal temperatures for their development inside shaded mines during extreme climatic conditions, whereas larvae in exposed mines were overheating, leading to major risks of mortality.

5. Tree canopies act as both magnifiers and reducers of the climatic regime experienced in open air outside canopies. Favourable and risky spots within the canopy do change as a function of the climatic conditions at the regional scale. The shifting nature of the mosaic of suitable and risky habitats may explain the observed uniform distribution of leaf miners within tree canopies.

Key-words: absorbance, lethal temperature, *Phyllonorycter blancardella*, stomatal conductance, thermal environment.

Journal of Animal Ecology (2007) **76**, 424–438
doi: 10.1111/j.1365-2656.2007.01231.x

Correspondence and present address: Sylvain Pincebourde. University of South Carolina, Department of Biological Sciences, Columbia, SC 29208, USA. E-mail: sylvainp@biol.sc.edu

Introduction

A huge number of studies have demonstrated the effects of body temperature on physiology and behaviour of ectothermic organisms (e.g. reviewed by Chown & Nicolson 2004). One remaining major gap in our knowledge, however, is a quantitative analysis of body temperatures experienced by organisms under natural conditions (Helmuth 2002). This lack of knowledge severely curtails the possibility to extrapolate from controlled physiological measurements to the organismal physiology in the field. The temperature of organisms often differs greatly from that of their surrounding, and usually results from the interaction between multiple climatic factors and physiological and physical properties of the organism (Gates 1980; Casey 1992; Helmuth 2002).

Quantification of body temperature in the field permits us to forecast the impacts of predicted climate change on organismal physiology. Quantitative studies based on continuous records of body temperatures and climatic variables are constrained by two experimental aspects. First, body temperature measurements of small and moving animals in the wild are challenging. Secondly, continuous measurements are often carried out during relatively small time windows. Fortunately, the biophysical approach mitigates these constraints because it does not only generate body temperature estimates using climatic data, but also it identifies the physical and physiological mechanisms that determine the body temperature patterns (e.g. Porter & Gates 1969; Helmuth 1998; Helmuth, Kingsolver & Carrington 2005; Pincebourde & Casas 2006a). Once the thermal mechanisms are elucidated, biophysical models can be used to extrapolate the shifts in body temperature in response to the climate change (e.g. Gilman, Wethey & Helmuth 2006).

A crucial step in our understanding of the impact of environmental conditions on organismal physiology is to quantify the spatial heterogeneity in microclimatic conditions at local scales (i.e. the spatial scale at which the organism is moving). Local heterogeneity in microclimatic conditions can be due to the interaction between the sun course and the ground topology, the environmental geometry, or the heterogeneity in surface material properties (e.g. Huey *et al*. 1989; Grace 1991; Weiss *et al*. 1993; Coxwell & Bock 1995; Helmuth 2002). It is therefore necessary to elucidate the mechanisms leading to the observed local heterogeneity in microclimate to obtain a comprehensive and realistic representation of the environment experienced by an organism.

A tree canopy is a highly heterogeneous environment (Orians & Jones 2001). The energy budget of a leaf differs from that of another one depending on its position within the canopy due to variations in radiation interception and wind attenuation. The amount of radiation a leaf receives strongly depends on the radiation level above the tree and on the quantity of radiation intercepted, reflected and transmitted by the neighbouring leaves. The light environment of a canopy results from the complex interaction between sun position, the amount of radiation at the top of the canopy, and the geometry of the canopy (e.g. Ackerly & Bazzaz 1995; Sinoquet *et al*. 1998, 2001; Montgomery & Chazdon 2001). Wind speed is attenuated when air flow penetrates the canopy. Wind speed attenuation depends on the total amount of foliage along the wind vector (Daudet *et al*. 1999).

The mechanistic relationship between canopy geometry, microclimate heterogeneity and the physiology of herbivore insects has never been explored in depth. Our aim is to elucidate these links, and to integrate them into biophysical models to predict body temperature patterns from climatic variables taken at the regional scale (i.e. above the tree) for any location within the habitat. This framework is then used to determine the spatial and temporal thermal heterogeneities in a phytophagous insect microclimate at the tree canopy scale, and the consequences for the insect's physiology.

We investigated the impact of local climate on microclimate, body temperature and larval developmental rate heterogeneities at tree canopy scale in the leaf mining moth *Phyllonorycter blancardella* (Fabricius 1781) (Lepidoptera: Gracillariidae). This moth infests all parts of apple tree canopies (Pottinger & LeRoux 1971; Casas 1990). We first elucidated the impact of climatic conditions on mine temperature patterns based on field measurements made during 4 days. From these field observations, we analysed the dynamics of the climate-dependent mosaic of optimal and suboptimal microclimates within tree canopies during moderate climatic conditions. Secondly, we explored the impacts of climate variability on microclimate and developmental rate heterogeneities at canopy scale under severe thermal conditions. For this purpose we built a model by integrating (1) a model for radiation and leaf energy balance distribution within a tree canopy (Sinoquet *et al*. 2001); (2) a biophysical model of mine temperature (Pincebourde & Casas 2006a); (3) an empirical model of larval body temperature (Pincebourde & Casas 2006b); and (4) a physiological model of larval developmental rate (Logan *et al*. 1976). This integration allows us to determine the developmental rate of a larva at a given location within the tree crown from climatic variables measured above the tree (i.e. regional climate) and tree canopy geometry. We tested the integrated model using the field temperature measurements. While the integrated model was found adequate for modelling microclimate temperatures during moderate climatic conditions, we do not know its behaviour and consequences under warm and hot regional climatic weather. Therefore, we used climatic data measured near our study site during the 2003 European heat wave to explore these aspects. Heat waves are extreme climatic events characterized by exceptionally hot air temperatures. They are likely to occur with an increasing frequency and duration during the next century in North America and Europe as a result of anthropogenic greenhouse gas accumulation in the atmosphere (Easterling *et al*. 2000; Seneviratne *et al*. 2006).

Methods

INSECT–PLANT RELATIONSHIP

The spotted tentiform leaf miner *Phyllonorycter blancardella* feeds on apple leaves. Females lay eggs individually on the lower side of leaves. Newly hatched larvae penetrate the leaf and five larval stages develop within leaf tissues. During the first three stages larvae are sap feeders, whereas the two last stages are tissue feeders (Pottinger & LeRoux 1971). Third stage larvae delimit the perimeter of the mine inside which fourth and fifth stage larvae feed on mesophyll tissues. The white spots at the mine surface (*c.* 1 cm^2) correspond to eaten areas, and the green patches correspond to the photosynthetically active tissues remaining within a mine (Pincebourde *et al*. 2006). A detailed description of the mine structure is given in Pincebourde & Casas (2006a). Our study focused on the fifth larval stage for which leaf tissue modifications are more pronounced (Pincebourde 2005; Pincebourde & Casas 2006a). The parameters related to stomatal behaviour and optical properties of the mine during the other larval stages are still unknown.

Temperature and climatic measurements, as well as determination of some model parameters, were made in the field. The canopy geometry of a 20-year-old apple tree *Malus communis* (L.) was measured in Vouvray (France), near Tours (47°22′N, 0°40′E). The tree was located in an open area. Its trunk had a circumference of 77 cm and a diameter of 25 cm. Its canopy was approximately 4·8 m in height, and 4·1 m and 4·9 m in east–west and north–south directions, respectively. The leaf miner was present at a low population density in the area. The apple tree was artificially infested with the leaf mining moth in June 2004. Fifteen bags made of fine tissue were placed at different locations within the tree crown, each bag enclosing a part of a branch. Some pupae and adults of the leaf miner, coming from our laboratory rearing, were dispersed within each bag.

MEASUREMENT OF CLIMATIC VARIABLES AND LEAF AND MINE TEMPERATURES

Leaf and mine temperature patterns were measured in the field on the 20-year-old apple tree in August 2004. Leaf and mine temperatures and climatic variables were measured simultaneously during four consecutive days (thereafter day 1, day 2, day 3 and day 4) showing different climatic conditions. These 4 days were categorized based on sky overcast. Two days (days 1 and 2) were cloudy (i.e. low radiation level and high ratio diffuse/direct radiation), whereas the two others (days 3 and 4) were sunny, cloudless days (i.e. high radiation level and low ratio diffuse/direct radiation).

Climatic measurements

Several instruments were deployed in the field. Air temperature and relative humidity within the canopy were measured using a MP100A probe (Campbell Scientific Ltd, Leicestershire, UK) equipped with a 41004-5 radiation shield (Campbell Scientific Ltd) and connected to a CR10X data logger (Campbell Scientific Ltd). The probe was placed 1·50 m above the ground within the canopy. Wind velocity and radiation level were measured above the canopy by placing the instruments 5 m above the ground near the apple tree. Wind velocity was recorded using a air velocity transducer (model 8465, TSI Incorporated, St Paul, MN, USA) connected to a CR10X data logger. Global radiation, diffuse radiation and PAR levels were measured with two pyranometer sensors (CM3, Campbell Scientific Ltd), the second being equipped with a shadow ring (CM 11/121, Kipp and Zonen, Delft, the Netherlands), and a quantum sensor (LI-190SA, Li-Cor Inc., Lincoln, NE, USA), respectively. The two pyranometers were connected to a CR10X data logger and the quantum sensor was linked to a LI-1400 data logger (Li-Cor Inc.). All measurements were made simultaneously every 5 min.

Leaf and mine temperature measurements

Leaf temperature was measured using a fine copper-constantan thermocouple (type T, 0·2 mm in diameter; TCSA, Dardilly, France) placed along the midrib and applied to the lower leaf surface. Thermocouples were attached such that the natural orientation of the leaves was not altered. Measurements were taken every 5 min. A total of 24 shaded leaves and 28 sunny leaves were measured during the 4 days, and different leaves were taken each day. The sample size differed due to exclusion from the analysis of some leaves showing an unclipped thermocouple during the day. Mine temperature was measured by inserting a fine copper-constantan thermocouple (type T, 0·2 mm in diameter; TCSA) through a feeding window located on the upper mined leaf surface. The insertion point was covered with vegetable oil in order to avoid any leakage. This method does not alter the stomatal behaviour in the lower mined leaf tissues (Pincebourde & Casas 2006a). Measurements were taken at 5-min intervals. Different mines were recording each day. Temperature measurements of 39 shaded mined leaf tissues and 28 sunny mined leaf tissues were obtained over the whole period and different mines were taken each day. Sample size differed for the same reasons as above. All thermocouples (leaves and mines) were connected to a Campbell CR10X data logger. All measured leaves and mines were labelled to identify them within the data set describing the canopy geometry, which allowed us to test for the accuracy of the integrated model (see below).

MODELLING RADIATION INTERCEPTION BY A CANOPY

The RATP model (Radiation Absorption, Transpiration and Photosynthesis) was designed to describe the spatial distribution of radiation, transpiration and

photosynthesis within plant canopies. The full model is described in Sinoquet *et al*. (2001) (see also Appendix S1, Supplementary material). Here, the submodel simulating the interception of solar radiation by leaves at the intracanopy scale was used. The model is based on the Beer's law, the canopy being treated as a turbid medium. This approach has been widely used to describe the light distribution within canopies (e.g. Impens & Lemeur 1969; Sinoquet & Bonhomme 1992; Kitajima, Mulkey & Wright 2005). Inputs for this model are the canopy geometry, optical properties of leaves and soil surface and the climatic driving variables. The canopy geometry is described by discretizing the space into a grid of 3D cubic cells (voxels) the size of which is user-defined. Each cell might be empty or characterized by the area density of a given plant component (i.e. leaf), according to 3D digitizing data. This model for interception of solar radiation was computed for both photosynthetically active radiation (PAR, 400–700 nm waveband) and near infrared radiation (NIR, 700–2500 nm waveband). Outputs are fluxes of PAR and NIR intercepted by both sunlit ($I_k^{sun,PAR}$ and $I_k^{sun,NIR}$, respectively) and shaded areas ($I_k^{shade,PAR}$ and $I_k^{shade,NIR}$, respectively) in each 3D cell k occupied by leaves.

MODELLING THE ENERGY BUDGET OF A LEAF AND OF A MINE

We used published biophysical models to compute the energy balance of leaves and mines (Campbell & Norman 1998; Nobel 1999; Pincebourde & Casas 2006a). Computing the energy budget of leaves is needed due to the leaf temperature dependence of the mine thermal environment. Briefly, the biophysical model computes heat fluxes exchanged through radiation absorbance, radiation emission, conduction–convection and evaporation mechanisms (Appendix S1). The energy balance was solved for temperature using the iterative Newton–Raphson method (Nougier 1985). These energy budgets were coupled with the model for interception of solar radiation described above. Outputs of the energy budget model are temperatures of both leaves and mines in sunlit (T_{Lk}^{sun} and T_{Mk}^{sun}, respectively) and shaded areas (T_{Lk}^{shade} and T_{Mk}^{shade}, respectively) within each 3D cell k of the canopy.

MODELLING LARVAL BODY TEMPERATURE

Body temperature of a larva in cell k (T_k^{body}) depends on mine temperature and larval position i within a mine. A larva experiences different temperature when below feeding windows that transmit radiation within a mine easily or when it is located below green patches that transmit radiation only weakly (Pincebourde & Casas 2006b). We used an empirical model to calculate body temperature in cell k and position i from the mine temperature and the amount of incoming radiation (Pincebourde & Casas 2006b). In the sunlit area (the same calculation hold for shaded area by using the radiation term for the shade), we have

$$T_{ik}^{body} = T_{Mk}^{sun} + f_i^{body}(I_k^{sun,PAR}) \quad \text{eqn 1}$$

where $f_i^{body}(I_k^{sun,PAR})$ is the empirical function describing the body-to-mine temperature deviation as a function of irradiance at larval position i within the mine. This function is, for feeding windows (FW) and green patches (GP), respectively,

$$f_{FW}^{body} = (0{\cdot}0034 I_k^{sun,PAR}) + 0{\cdot}0293 \quad \text{eqn 2}$$

$$f_{GP}^{body} = (0{\cdot}0013 I_k^{sun,PAR}) - 0{\cdot}017 \quad \text{eqn 3}$$

These empirical relationships were obtained using metal halide lamps to irradiate the mines and the insects (see Pincebourde & Casas 2006b). The light spectrum of these lamps is very similar to that of the sun, including the ratio visible to near infrared radiation. The entire solar spectrum is therefore implicitly considered into the empirical eqns 2 and 3.

Data reported by Djemai, Meyhöfer & Casas (2000) show that, on average, 40% of the body is positioned below feeding windows, whereas 60% is not. Body temperature was therefore calculated as a weighed average of body temperatures found at the two locations. Outputs of the model at this stage are therefore body temperature of fifth stage larvae, within sunlit and shaded mines, in cell k.

MODELLING LARVAL DEVELOPMENTAL RATE

Developmental rate is defined as the inverse of the developmental time. The model developed by Logan *et al*. (1976) was used to compute the instantaneous developmental rate (dT: h^{-1}) of a larva as a function of body temperature in cell k averaged over an hour

$$dT_k = C_1 \left[\exp(C_2(T_{ik}^{body} - T_{low}^{thr})) - \exp\left(C_2(T_{up}^{thr} - T_{low}^{thr}) - \frac{T_{up}^{thr} - T_{ik}^{body}}{C_3} \right) \right] \Big/ 24 \quad \text{eqn 4}$$

where T_{low}^{thr} and T_{up}^{thr} are lower temperature threshold for development and upper lethal temperature (°C), respectively. C_1 (day^{-1}) is the developmental rate at the lower threshold; C_2 is the rate of increase from the lower temperature threshold to optimum temperature for development; and C_3 (°C) is the temperature range over which an increase in temperature has a negative influence on the developmental rate (e.g. see Fig. 4 for a graphical representation of the model). Instantaneous developmental rate was obtained dividing by 24 the equation that was initially developed to compute the daily developmental rate. We also computed the daily developmental rate (day^{-1}), which is defined as the development rate per day. It was computed by summing

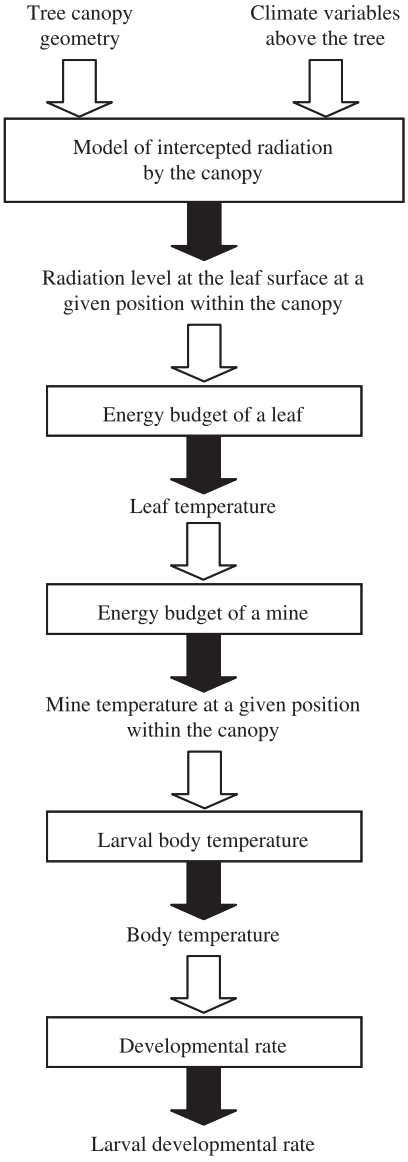

Fig. 1. The conceptual approach. This scheme shows how the radiation interception model, the energy budget models, the model of body temperature and the physiological model of developmental rate were integrated such that the larval developmental rate was predicted from regional climatic data (i.e. above the tree) and canopy geometry parameters. Boxes indicate the models, white arrows the model entries, and black arrows the model outputs.

the instantaneous developmental rates over the entire day. This physiological model assumes instantaneous adaptation of body temperature and also assumes that the developmental rate is independent of the temperatures previously sustained by the larvae.

CROSSING SPATIAL SCALES

The radiation interception model, the energy budget models, the model of body temperature and the physiological model of developmental rate were combined in a final step (Fig. 1). This combination allowed us to calculate instantaneous and daily developmental rates of a larva located inside a given mine on a given leaf at a given location within the tree canopy, from the regional climatic data and the canopy geometry parameters. The complete model is called afterward 'integrated model'. The integrated model comprises therefore a biophysical (mechanistic) component (radiation interception model and energy budgets), a physiologically semimechanistic part (developmental rate), and an empirical (nonmechanistic) component (body temperature model). The radiation interception model and the energy budgets of a leaf and a mine have been previously tested individually (Sinoquet *et al*. 2001; Pincebourde & Casas 2006a). Hence, we tested here the biophysical model combining the two using the data of leaf and mine temperatures and climatic variables measured during moderate climatic conditions. We did not test the body temperature, instantaneous developmental rate and integrated models in the field because it is impossible to measure body temperature without opening and destroying the mine.

MODEL PARAMETERS

Parameters of the models are described in Table 1.

Parameters for the radiation interception model

Canopy geometry was measured with a 3D digitizer and the software Pol95 (Adam 1999), which capture localization in the space (3D coordinates) and orientation (three angles of Euler) of each leaf within a tree crown (Sinoquet *et al*. 1998). Dimensions of the leaves were also partly measured and the distribution of leaf dimensions was used to model those of the unmeasured leaves. Our data set reports the spatial description of a canopy containing 26 281 leaves and a total foliage area of 37·01 m^2 (Fig. 2). We described canopy geometry as a matrix of 3D cubic cells, the volume of which was 8000 cm^3 (i.e. 20 cm × 20 cm × 20 cm).

Parameters for the energy budgets

All the parameters used to compute net radiation and sensible heat (i.e. heat exchanged through conduction–convection) balances of both leaves and mines are given in Pincebourde & Casas (2006a). We measured the maximal stomatal conductance values to compute the latent heat (i.e. heat lost through evaporation) balance of a leaf and a mine. Maximal stomatal conductance of both intact and mined leaf tissues were measured using an infrared gas analyser–leaf chamber system (LI-6400, Li-Cor Inc.). Measurements were made *in situ* on the 20 years apple tree following the method explained in Pincebourde & Casas (2006a). Maximal stomatal conductance was recorded on 13 intact sunny leaves and on 19 sunny mined integuments. The stomatal responses to environmental changes are given in Pincebourde & Casas (2006a).

Table 1. Parameters of the integrated model. Equations of the stomatal response functions are given in Pincebourde & Casas (2006a)

Parameters	Symbols	Values (units)	Sources*
Climatic variables			
Incident global radiation	I_{bo}	0–1161·1 W m^{-2}	Driving variable
Incident diffuse radiation	I_{do}	0–193·3 W m^{-2}	Driving variable
Air temperature	T_{air}	15·6–36·8 °C	Driving variable
Ground temperature	T_g	21 °C	Driving variable
Air relative humidity	hr	40–70%	Driving variable
Air vapour pressure deficit	e_a	957·9–2967·7 Pa	Driving variable
Wind velocity	u	0·4 m s^{-1}	Driving variable
Tree canopy geometry			
Leaf twist angle	θ	–180–180°	
Leaf inclination angle	α	–88·52–89·08°	
Leaf azimuth angle	ϕ	–180–180°	
X coordinate range	X	534·01 cm	
Y coordinate range	Y	491·48 cm	
Z coordinate range	Z	299·39 cm	
Absorbance			
Leaf PAR	a_L^{PAR}	0·84	Pincebourde & Casas (2006a)
Leaf NIR	a_L^{NIR}	0·02	Pincebourde & Casas (2006a)
Mine PAR	a_M^{PAR}	0·48	Pincebourde & Casas (2006a)
Mine NIR	a_M^{NIR}	0·44	Pincebourde & Casas (2006a)
Soil scattering coefficient			
Soil PAR	ρ_s^{PAR}	0·07	Combes *et al*. (2000)
Soil NIR	ρ_s^{NIR}	0·20	Combes *et al*. (2000)
Plant conductance			
Leaf upper surface	g_L^u	0·003 mol m^{-2} s^{-1}	Pincebourde *et al*. (2006)
Mine upper surface	g_M^u	0·009 mol m^{-2} s^{-1}	Pincebourde *et al*. (2006)
Leaf max. stomatal cond.	g_L^{max}	0·276 mol m^{-2} s^{-1}	
Mine max. stomatal cond.	g_M^{max}	0·227 mol m^{-2} s^{-1}	
Metric parameters			
Mine–leaf interface area	P_M	$1{\cdot}40 \times 10^{-5}$ m^2	Pincebourde & Casas (2006a)
Mine surface	S_M	$1{\cdot}02 \times 10^{-4}$ m^2	Pincebourde & Casas (2006a)
Developmental rate model†			
Lower threshold		5·2 °C	Baumgartner & Severini (1987)
Upper threshold		42 °C	
Lower development	C_1	0·047 day^{-1}	Baumgartner & Severini (1987)
Rate of increase	C_2	0·066	Baumgartner & Severini (1987)
Temperature range	C_3	2·390 °C	Baumgartner & Severini (1987)

PAR, photosynthetically active radiation; NIR, near infrared radiation; max., maximal; cond., conductance. *Data are from the current study except as noted. †Parameters of the developmental rate model of Logan *et al*. (1976) applied to last larval stage of *P. blancardella.*

Parameters for the developmental rate model

The developmental rate model was parameterized using both published data (Baumgartner, Delucchi & Genini 1981; Baumgartner & Severini 1987) and our own measurement of upper lethal temperature (T_{up}^{thr}). The temperature threshold inducing 50% mortality (LD_{50}) was measured by placing 10 groups of 12 freshly excised fifth stage larvae ($n = 120$ larvae) at a given temperature within a climatic chamber. The chamber regulated temperature with a 0·1 °C precision. For each group, the 12 larvae were placed within a small Petri dish equipped with a fine copper-constantan thermocouple (type T, 0·2 mm in diameter; TCSA) measuring the temperature inside the Petri dish. Air within the Petri dish was maintained saturated for water vapour by placing a humid cotton piece inside. Each group of 12 larvae was treated separately. The Petri dish was first placed at 30 °C for 15 min. The temperature was then increased by 0·32 °C per minute (i.e. rate of increase inherent to the climatic chamber) until it reached the pre-defined temperature. This temperature was maintained for 1 h after which the Petri dish was removed from the chamber. Each group was tested at a different experimental temperature from 36 °C to 45 °C (with 1 °C increment). Larval survival was assessed twice, immediately after the thermal treatment and 24 h later. The test consisted of touching larvae with a fine needle. Living larvae

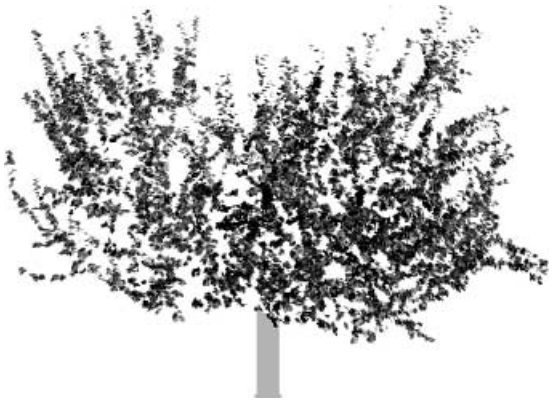

Fig. 2. 3D representation of the 20-year-old apple tree, when viewed from the south-west side (azimuth 120°). This representation was obtained using VegeSTAR software (Adam, Sinoquet & Dones 2001). Leaves were assimilated as polygon-shaped entities. Variations in grey levels correspond to variations in the amount of radiation received by leaves when the tree is exposed to direct radiations. The darker the leaves, the higher the amount of radiation intercepted. The trunk has been drawn for visual convenience.

moved violently under this treatment. This behaviour is the characteristic response to oviposition attempts by parasitoids (Djemai *et al*. 2000).

MODEL EXPLORATIONS

The temperatures of leaves and mines during two non consecutive clear days having similar radiation levels but differing in maximal air temperatures during daytime were simulated using the integrated model. We used meteorological data from the AGROCLIM database (INRA, France; [www.avignon.inra.fr/internet/unites/unite_experimentales/agroclim/version_index_html]) taken at Lusignan (France; 51°60′N, 0°15′E) on 20 and 22 June during the 2003 European heat wave. The first day ('warm day') was a typical summer day in the centre of France, whereas the second day ('hot day') was an extremely warm day. The loaded data consisted in values of air temperature and global incident radiation taken at a 1 h time step. The amount of diffuse radiation was theoretically determined using the ratio diffuse-to-global radiation, which depends on solar zenith angles (Gates 1980). PAR and NIR were assumed to contribute solar radiation by 48 and 52%, respectively (Varlet-Grancher 1975). The other meteorological variables were fixed at realistic values. The parameters in Table 1 were used for all simulations. A third of the leaves was assumed to be occupied by a mine for the simulation purposes and mined leaves were chosen by random within the 3D data sheet. Then, the number of cells occupied by mines, and therefore the sample size in the analysis, was 1611. Instantaneous developmental rates were obtained by using the body temperature predicted for each hour. We report leaf, mine and body temperature and developmental rates for 1611 grid cells of the canopy, which consisted in a total of 1943 cells.

STATISTICAL ANALYSES

Box plot charts were built to represent the temperature patterns measured in the field during the four moderate days in August 2004. The distributions were compared using a two-sided Kolmogorov–Smirnov test (KS). The combination of the radiation interception and the energy budget models (biophysical part of the integrated model) was tested by comparing predictions of leaf and mine temperature to measurements made in the field during the 4 days. The thermal heterogeneity of mine microclimate at canopy scale was compared with that of leaves by plotting the temperature deviation between sunny and shaded mines as a function of that of leaves. A Student's *t*-test was used to test for a difference between the slopes of the regression lines (Zar 1998). Regressions were set to go through the origin.

The model was run using the climatic data recorded continuously during the four moderate days. The biophysical model was tested for its accuracy by performing Pearson correlations between predictions and measurements and by calculating the root mean square error (RMSE) of the predictions from the 1 : 1 relationship (i.e. measured temperature equals predicted temperature).

Results

PARAMETER ESTIMATIONS

Canopy geometry

The total leaf area per class of leaf inclination angle was computed. Inclination angle ranged from –88·52° to +89·08°. An inclination angle of 0 °C means that the leaf is horizontally orientated and perpendicular to the solar beam when the sun is at the zenith position. The distribution of leaf area per class of leaf inclination angle was normal (Lillifors two-tailed probability test: $P = 0{\cdot}74$, nonsignificant from normal distribution). The distribution peaked at the inclination angle 0° and 22% of the canopy foliage had an inclination ranging from –10° to 10°.

Maximal stomatal conductance

The mean maximal stomatal conductance of mined leaf tissues ($0{\cdot}227 \pm 0{\cdot}108$ mol m^{-2} s^{-1}, $n = 19$) was similar to that of intact leaf tissues ($0{\cdot}276 \pm 0{\cdot}123$ mol m^{-2} s^{-1}, $n = 13$; Student's *t*-test: $P = 0{\cdot}71$).

Upper lethal temperature

All larvae survived at a body temperature of 38 °C but the survival rate continuously decreased above that temperature. All excised larvae were killed during an exposure of 1 h at a body temperature of 43 °C (Fig. 3). The LD_{50} was at body temperature 42 °C for an exposure of 1 h (Fig. 3). Thus, the body temperature range between about 38 °C and 42 °C was considered as the thermal stress temperature range in *P. blancardella*.

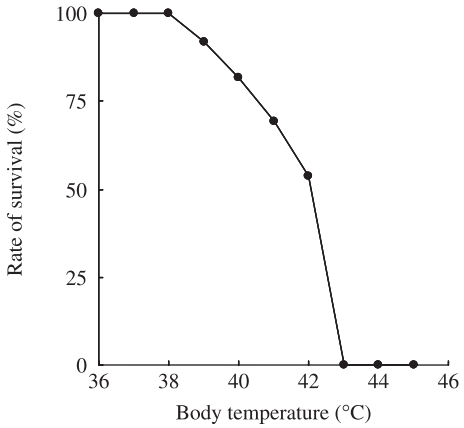

Fig. 3. Determination of the upper lethal temperature threshold for fifth stage *P. blancardella* larvae. Rate of survival is shown as a function of body temperature for an exposure of 1 h. Each dot represents a sample of 10 larvae.

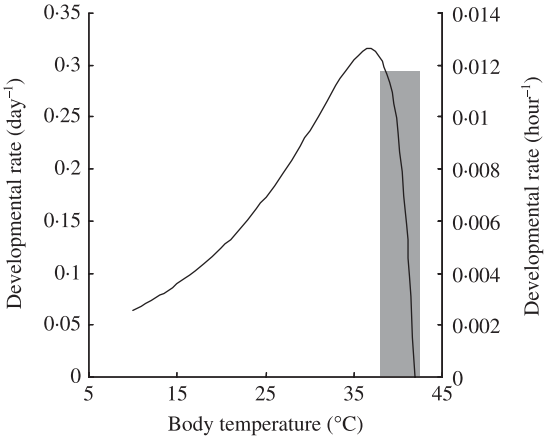

Fig. 4. The physiological model of developmental rate for fifth stage *P. blancardella* larvae. The developmental rate is shown as a function of body temperature on a daily (left axis) and on an hourly basis (right axis). The grey part of the curve indicates the body temperature range that induces thermal stress.

Developmental rate model

The development rate of larvae increases exponentially until body temperature reaches 37 °C, and decreases sharply from 37 °C to 42 °C (Fig. 4).

FIELD MEASUREMENTS: LEAF AND MINE TEMPERATURE PATTERNS

Temperature patterns during cloudy conditions

The climatic conditions during the two cloudy days ranged from 15·6 °C to 22·4 °C for air temperature, 57% to 91% for relative humidity, and 0 to 2·30 m s^{-1} for wind speed. Global and diffuse radiation levels were up to 883 W m^{-2} and 369 W m^{-2}, respectively, at midday. The maximal radiation levels were relatively

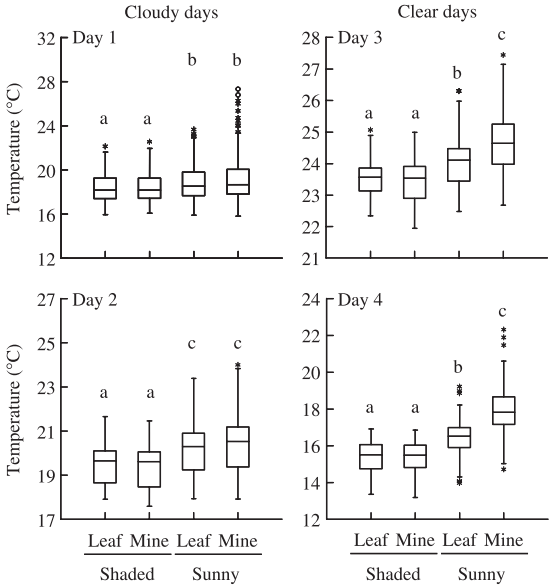

Fig. 5. Box plot charts of leaf and mine temperatures during two cloudy days (leaf panels) and two clear days (right panels) at both shaded and sunny locations. In each box plot, the centre horizontal line marks the median of the sample. The length of each box indicates the range within which the central 50% of the values fall with the box edges at the first and third quartiles. The whiskers show the range of values that fall within the inner fences. The asterisks indicate the values within inner and outer fences and far outside values are plotted with empty circles. Statistically different distributions are indicated by different letters above each box plot (two-sided Kolmogorov–Smirnov test).

high for a cloudy day, due to sun appearing for a very short time window (i.e. about 15 min). The temperature pattern of leaves and mines were similar during the two cloudy days at shaded locations (Fig. 5; KS test: day 1, $D = 0{\cdot}075$; day 2, $D = 0{\cdot}183$; $P > 0{\cdot}05$ for both) as well as at sunny locations (Fig. 5; KS test: day 1, $D = 0{\cdot}069$; day 2, $D = 0{\cdot}143$; $P > 0{\cdot}05$ for both). Temperature patterns, however, differed significantly between shaded and sunny locations for both leaves (Fig. 5; KS test: day 1, $D = 0{\cdot}167$; day 2, $D = 0{\cdot}371$; $P < 0{\cdot}001$ for both) and mines (Fig. 5; KS test: day 1, $D = 0{\cdot}179$; day 2, $D = 0{\cdot}497$; $P < 0{\cdot}001$ for both). This suggests that leaves and mines reached similar temperatures during cloudy conditions within the respective locations.

Temperature patterns during sunny conditions

Air temperature ranged from 12·1 °C to 24·7 °C, relative humidity from 66% to 88%, and wind speed from 0 to 3·2 m s^{-1} during the 2 days explored. Global and diffuse radiation levels were up to 1023 W m^{-2} and 362 W m^{-2}, respectively. The temperature pattern of leaves and mines were similar during the two clear days at shaded locations only (Fig. 5; KS test: day 3, $D = 0{\cdot}131$; day 4, $D = 0{\cdot}044$; $P > 0{\cdot}05$ for both). The temperature pattern of leaves and mines were different at sunny locations suggesting that sunny mines reached higher temperatures than sunny leaves under clear sky conditions (Fig. 5;

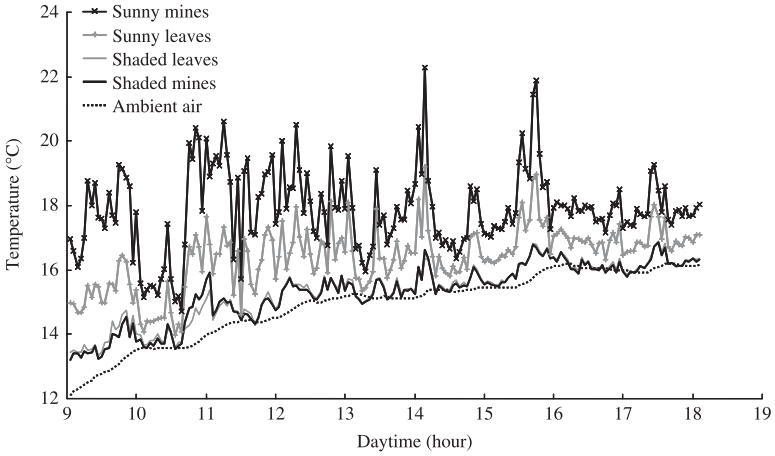

Fig. 6. Mean temperature of mines, leaves and ambient air measured during the day 4 (clear, sunny day). Sunny mines were always warmer than shaded mines and all leaves.

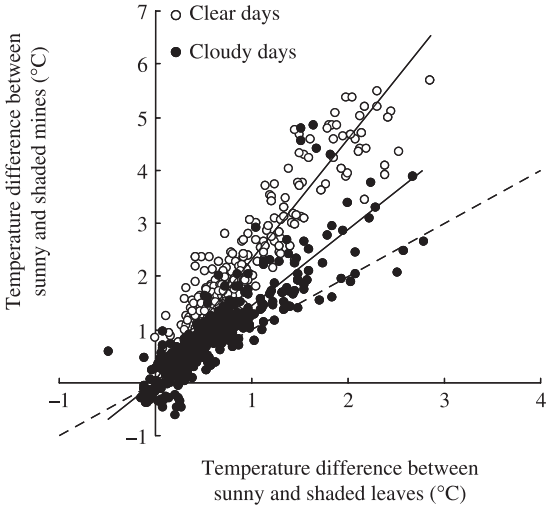

Fig. 7. Mine and leaf temperature heterogeneities at canopy scale during the cloudy and the clear days. The difference between mine temperature at shaded and sunny locations is given as a function of the difference between leaf temperature at shaded and sunny locations. The dashed line indicates the $x = y$ relationship (i.e. microclimate heterogeneity is similar for both mines and intact leaves).

KS test: day 3, $D = 0{\cdot}352$; day 4, $D = 0{\cdot}599$; $P < 0{\cdot}001$ for both). Temperature patterns differed significantly between shaded and sunny locations for both leaves (Fig. 5; KS test: day 3, $D = 0{\cdot}434$; day 4, $D = 0{\cdot}516$; $P < 0{\cdot}001$ for both) and mines (Fig. 5; KS test: day 3, $D = 0{\cdot}631$; day 4, $D = 0{\cdot}846$; $P < 0{\cdot}001$ for both). The temperature patterns measured during day 4 are given for illustrative purposes in Fig. 6. The temperature of sunny mines and leaves was highly variable due to variations in wind speed as well as in radiation level.

Comparing mine and leaf thermal heterogeneities at canopy scale

Thermal heterogeneity of leaf and mine microclimates at canopy scale were quantified by calculating the temperature difference between the sunny and the shaded locations for each category (leaf and mine) and for each set of climatic condition (clear vs. cloudy, cumulating the 2 days for each). The thermal heterogeneity of mines was higher than that of leaves during the two climatic conditions (Fig. 7). The thermal heterogeneity of mine microclimate was linearly related to that of leaf microclimate during the clear days (linear regression, $y = 2{\cdot}29x$, $R^2 = 0{\cdot}86$, $P < 0{\cdot}001$) as well as during the cloudy conditions (linear regression, $y = 1{\cdot}43x$, $R^2 = 0{\cdot}76$, $P < 0{\cdot}001$) (Fig. 7). However, the slope of the two regression lines significantly differed (Student's t-test: $P < 0{\cdot}001$) and their values indicated that the thermal heterogeneity of the mine microclimate was increased by 129% and 43% during clear and cloudy climatic conditions, respectively, when compared with that of the leaf microclimate at canopy scale.

VALIDITY OF THE INTEGRATED MODEL

Testing the validity during cloudy conditions

Model predictions for shaded leaf temperature were well matched by measurements in the field (day 1: Pearson's $r = 0{\cdot}84$; day 2: Pearson's $r = 0{\cdot}95$; $P < 0{\cdot}001$ for both) as for sunny leaf temperature (day 1: Pearson's $r = 0{\cdot}87$; day 2: Pearson's $r = 0{\cdot}91$; $P < 0{\cdot}001$ for both) (Fig. 8). Model predictions for shaded and sunny mine temperature were also matched by measurements (shaded mines: Pearson's $r = 0{\cdot}89$ for day 1, and Pearson's $r = 0{\cdot}96$ for day 2; sunny mines: Pearson's $r = 0{\cdot}91$ for day 1, and Pearson's $r = 0{\cdot}88$ for day 2; $P < 0{\cdot}001$ for all) (Fig. 8). The average RMSE of predictions for shaded leaves, sunny leaves, shaded mines and sunny mines were (day 1/day 2) 0·88 °C/0·52 °C, 0·75 °C/0·86 °C, 0·66 °C/0·36 °C and 0·97 °C/1·19 °C, respectively. The RMSE of predictions for the two whole data sets was 0·82 °C and 0·73 °C, respectively. Therefore, the biophysical model adequately predicts both leaf and mine temperatures as a function of their location within the canopy during cloudy conditions.

Testing the validity during sunny conditions

Model predictions for leaf and mine temperatures were matched by measurements (day 3: shaded leaves: Pearson's $r = 0{\cdot}86$; sunny leaves: Pearson's $r = 0{\cdot}83$; shaded mines: Pearson's $r = 0{\cdot}91$; sunny mines: Pearson's $r = 0{\cdot}93$; day 4: shaded leaves: Pearson's $r = 0{\cdot}96$; sunny leaves: Pearson's $r = 0{\cdot}82$; shaded mines: Pearson's $r = 0{\cdot}93$; sunny mines: Pearson's $r = 0{\cdot}80$; $P < 0{\cdot}001$ for all; Fig. 8). The average RMSE of predictions for shaded leaves, sunny leaves, shaded mines, sunny mines and the whole data set were (day 3/day 4) 0·42 °C/0·48 °C, 1·01 °C/0·56 °C, 0·52 °C/0·74 °C, 0·95 °C/0·87 °C and 0·73 °C/0·66 °C, respectively. The biophysical model at canopy scale predicts leaf and mine temperatures with acceptable precision under clear sky conditions.

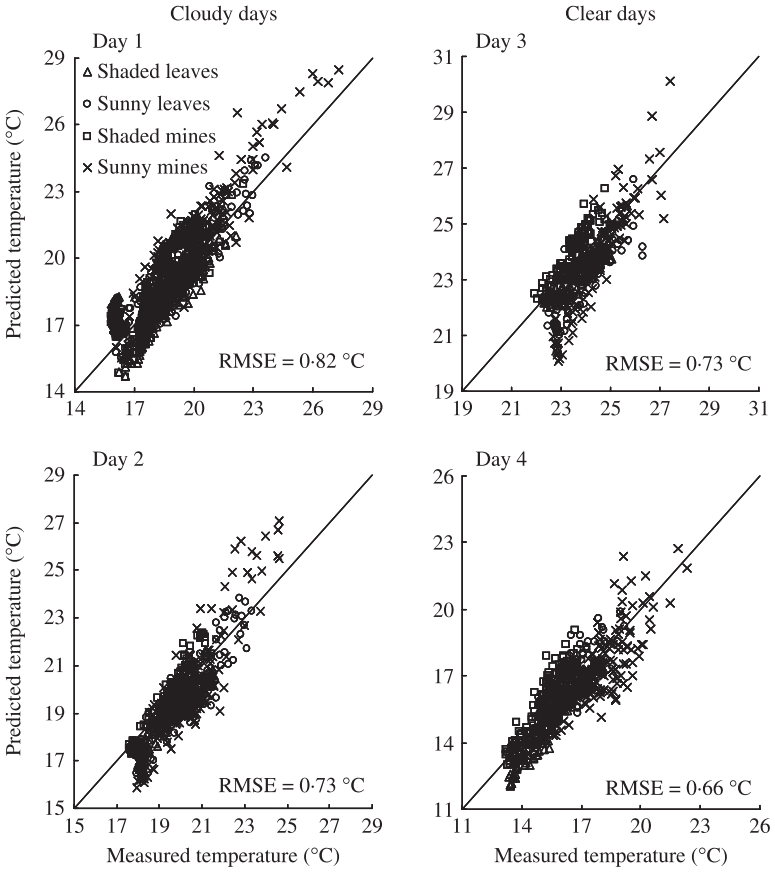

Fig. 8. Accuracy of the integrated model as shown by comparing its predictions and actual records of leaf and mine temperatures, made at several positions within the tree canopy and during moderate climatic conditions. This comparison was done for both cloudy conditions (left column) and sunny conditions (right column). Lines show the $x = y$ relationship and the root mean square error of predictions (RMSE) is given for the whole data set of each day.

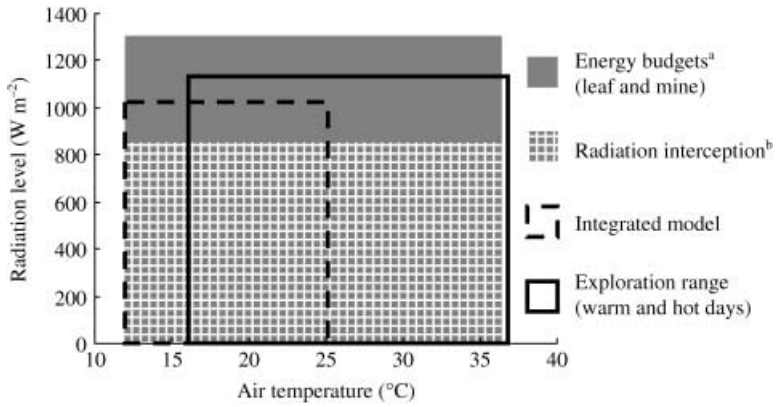

Fig. 9. Range of air temperature and radiation level over which the energy budgets models (both leaf and mine), the radiation interception model and the integrated biophysical model were tested. Each area on the graph comprises all variable values tested for each model. All models were found to be valid within the range of climatic conditions tested. The range of variables used for the model explorations is also indicated. Superscript letters indicate the models that were tested elsewhere: [a]Pincebourde & Casas (2006a); [b]Sinoquet *et al*. (2001).

Range of validity

The energy budgets of a leaf and a mine and the radiation interception model were previously tested over a wide range of radiation and air temperature values (Sinoquet *et al*. 2001; Pincebourde & Casas 2006a; Fig. 9). The integrated biophysical model was tested over a smaller range in the field (Fig. 9). All models were found to be valid within the range of climatic conditions tested. The model exploration range (corresponding to the moderate and the hot days) included the integrated model testing range and beyond that (Fig. 9). Our predictions are, however, likely to be valid as (1) the exploration range is within the range of validity of the individual models, and (2) the integrated model was valid over the entire range tested and there were no signs of divergence between data and predictions at the boundaries of the tested parameter range.

MODEL EXPLORATION: PATTERNS OF LEAF, MINE AND BODY TEMPERATURE

The radiation level pattern during the warm and the hot days were very similar, with a maximal level at midday of 1139 W m^{-2} and 1111 W m^{-2}, respectively (Fig. 10a,b). Air temperature was the only meteorological variable which differed between the two days. Maximal air temperatures were 29·1 °C and 36·8 °C during the warm and the hot days, respectively (Fig. 10c,d). We summed the sunny foliage area of all grid cells to compute the amount of canopy foliage directly exposed to solar radiation. We found that about 44% of the total foliage area was directly exposed to the sun between 7.00 and 17.00 h (not shown). Therefore, the sunny habitat was a significant proportion of the canopy.

The same general pattern of leaf and mine temperature was found for the 2 days (Fig. 10c,d). Sunny categories were always warmer than shaded categories. Shaded mines were warmer than shaded leaves during daytime, and the temperature of sunny mines was always higher than that of sunny leaves. The standard deviations of mean temperatures in sun and shade at a given time were relatively low and ranged from 0·40 °C to 0·86 °C during the warm day and from 0·51 °C to 1·09 °C during the hot day (minimum to maximum, taken over the daytime and over all locations; not shown).

Body temperature of larvae within sunny mines was predicted to be well below the temperature range inducing thermal stress during the warm day (Fig. 10c). The mean temperature within sunny mines was up to 35·0 °C at midday during the warm day, and mean body temperature was up to 36·4 °C, which is very close to the optimal temperature for development. The mean temperature within shaded mines was only 28·7 °C at midday during warm conditions (Fig. 10c). The mean body temperature within shaded mines was less than 0·5 °C above mine temperature (not shown). Indeed, mean body temperature within shaded mines was about 8 °C below the optimal temperature for larval

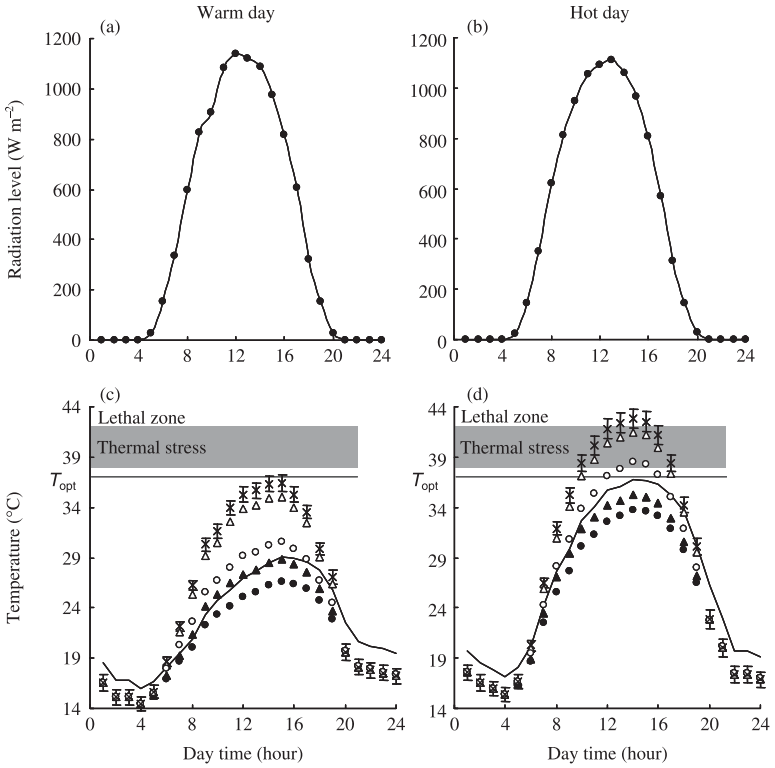

Fig. 10. Radiation level is shown during the warm (a) and the hot (b) day. Integrated model predictions (means, SD not shown for clarity) of leaf and mine temperatures at shaded and sunny locations, and measured air temperature, are given for the warm (c) and the hot (d) day. Mean (± SD) body temperature of larvae within sunny mines is also shown. The mean body temperature of larvae within shaded mines was very close to the microclimate temperature (not shown for clarity). The grey parts indicate the body temperature range that induces thermal stress. Temperatures above the stressful range are lethal (at an exposure of 1 h). The horizontal lines indicate the optimal temperature for larval development (T_{opt}). Legends (c and d): air temperature (—), shaded leaf (●), sunny leaf (○), shaded mine (▲), sunny mine (△), body temperature (×).

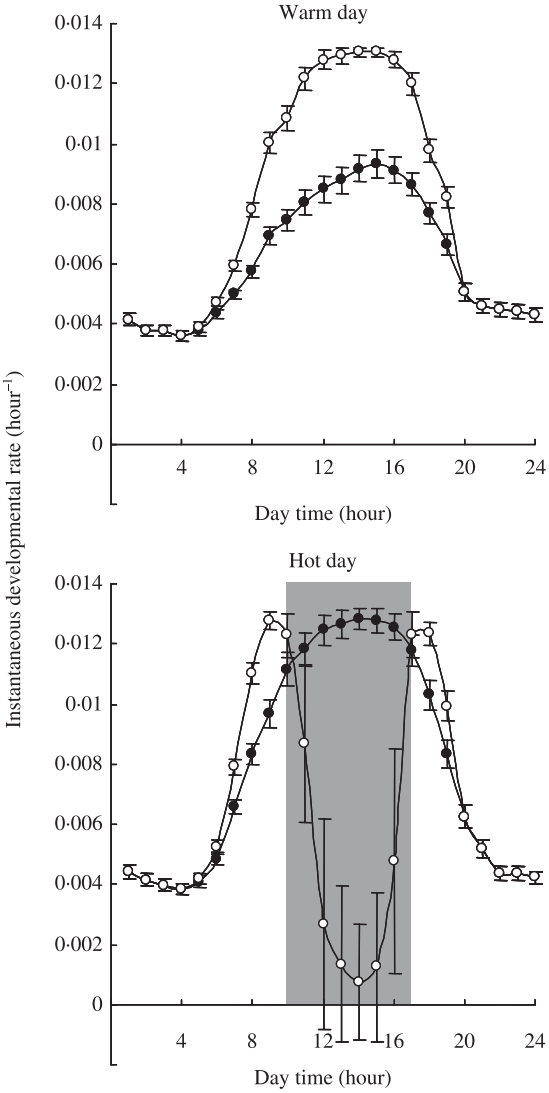

Fig. 11. Instantaneous developmental rate of fifth stage *P. blancardella* larvae within sunny (○) and shaded (●) mines during the warm and hot days (mean ± SD). Thermally stressful period as deduced from body temperature patterns is indicated in grey for sunny mines.

development. Mean shaded mine temperature, however, was up to 35·3 °C during the hot day, bringing body temperature close to the optimal level for their development (Fig. 10d). By contrast, mean sunny mine temperature during the hot day was within the thermal stress range for about 7 h (Fig. 10d). Mean sunny mine temperature and mean body temperature of larvae living inside were up to 41·5 °C and 42·9 °C, respectively, at midday. Thermal conditions within sunny mines are therefore dangerous for the leaf miner during a hot day.

MODEL EXPLORATION: HETEROGENEITY IN DEVELOPMENTAL RATES

Not surprisingly, the instantaneous developmental rate of larvae within sunny mines was higher than that within shaded mines during the warm day (Fig. 11). For example, the mean instantaneous developmental rate within sunny mines at 14.00 h was increased by 42% when compared with that within shaded mines. The instantaneous developmental rate in sunny mines during the hot day showed a different pattern. Instantaneous developmental rate within sunny mines was 94% lower than that within shaded mines at about 14.00 h, when the sunny mine temperature attained its maximal value (Fig. 11).

These differences in instantaneous developmental rates between sunny and shaded locations resulted in variations in daily developmental rates. The daily developmental rate within sunny mines was significantly increased by 28% when compared with that in shaded mines during the warm day (Student's *t*-test: $t_{1610} = 1208{\cdot}4$, $P < 0{\cdot}001$) (Fig. 12a). By contrast, the daily developmental rate within sunny mines was 22% lower during the hot day when compared with that in shaded mines (Student's *t*-test: $t_{1610} = 84{\cdot}8$, $P < 0{\cdot}001$) (Fig. 12a). Body temperature within sunny mines was above 42 °C for more than 1 h in 81·2% of the 1611 grid cells. The lethal exposure was never reached within the 18·8% grid cells remaining.

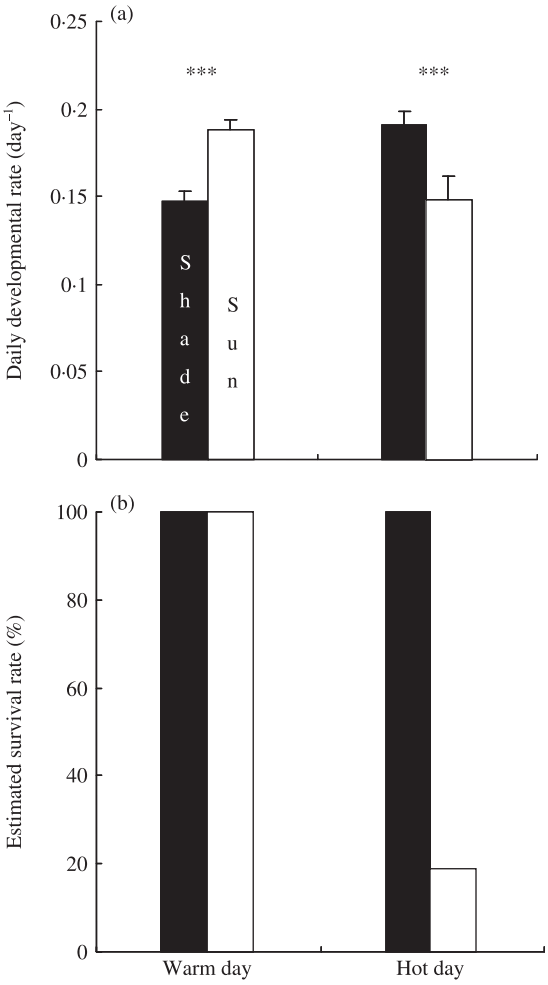

Fig. 12. Daily developmental rate (a) (mean ± SD) and estimated survival rates (b) of fifth stage *P. blancardella* larvae within sunny (white bars) and shaded (black bars) mines during the warm and the hot days. Survival rate was deduced from the proportion of larvae having a body temperature warmer than 42 °C for at least 1 h during the day. Stars indicate the level of statistical significance ($P < 0{\cdot}001$).

This suggests that a temperature-induced mortality rate of about 81% could arise within sunny mines during the hot day conditions (Fig. 12b). By contrast, we predicted from temperature patterns that the survival rate would be 100% within all mines during the warm day and within shaded mines during the hot day (Fig. 12b).

Discussion

VALIDITY AND GENERALITY OF THE MODEL

We combined two biophysical models (radiation interception by canopies and energy budgets) to compute microclimate temperatures from regional climatic data. The possibility that errors of each model may interact is of concern. Estimating the potential level of this error is therefore critical when interpreting the model outputs. The radiation interception model was shown by Sinoquet *et al*. (2001) to accurately predict both the magnitude and the daily course of leaf irradiance with a root mean square error of predictions of 90 μmol m^{-2} s^{-1}. Moreover, the energy budget of a mine has been shown to predict mine temperature with a root mean square of prediction of 0·9 °C (Pincebourde & Casas 2006a). The temperature change induced by a variation in irradiance of 90 μmol m^{-2} s^{-1} causes a temperature change of less than 1 °C. The predicted worse error of the integrated model is obtained by summing the error of each model (because the two models are independent from each other), i.e. less than 2 °C. The largest measured error of the integrated model was obtained for sunny mine temperature, which was overestimated up to about 1 °C. Therefore, combining several models does not disproportionately increase the error of predictions. An error of 1 °C could, however, still be problematic when body temperatures are close to the lethal level, as adding or subtracting 1 °C to the mean body temperature in sunny mines during the hot day leads to an estimated mortality rate of 95% and 49%, respectively. The mortality rate due to physical conditions is, however, expected to be significant in any case.

The integrated model works on the basis of the amount of radiation intercepted by a given leaf. It categorizes a leaf or a mine into sunny or shaded locations. Thus, we concentrate here on the two extreme microclimates to determine the boundaries of the thermal heterogeneity at the canopy scale, i.e. leaves that are always under the sun and those that are in the shade throughout the day. A single leaf within the canopy can, however, shift between a sunny and a shaded microclimate within the same day, depending on its position within the tree crown. For example, leaves located in the periphery of East and West portions of a large and spatially complex canopy can receive radiation only early in the morning and late in the afternoon, respectively (Sinoquet *et al*. 2001). Canopy gaps can also cause some shaded leaves at the bottom of the tree crown to receive radiation for short time windows (Sinoquet *et al*. 2001). Moreover, the radiation interception model computes the amount of radiative energy absorbed by each leaf by averaging the leaf inclination angle within each cell k. The true variability in leaf and mine temperatures is therefore higher than computed from the mean inclination angle. A leaf absorbs more solar energy when the inclination angle is 0° (i.e. the leaf surface is perpendicular to solar beam) and then declines as the inclination angle decreases or increases. Leaves and mines having a large inclination angle would likely experience a thermal environment that is intermediate between the sunny and shaded location. We observed a normal distribution of leaf area as a function of leaf angle for the whole canopy with the distribution peak at inclination angle of about 0°. The results we report are therefore representative of what is happening for most leaves and mines within a canopy.

The sheer amount of work needed to map more than 26 000 leaves, as well as the difficulties of the best stochastic and statistical models for plant canopy structure to predict the geometry dynamics in older trees (e.g.

Costes *et al*. 2003; Durand *et al*. 2005) implies that we are not yet in a position to consider the impact of varying canopy geometry on the microclimate experienced by insects. However, the rather dense canopy structure of our tree, combined with the uniform distribution of leaf miners implies that we have broadly sampled all possible microclimatic regimes. Such models as the one we propose are actually necessary to describe the intracanopy distribution of microclimate and developmental rate. For example, it is impossible to compute the developmental rates solely from mine temperature measurements as both the amount of radiation received and body temperature are unknown for all locations.

BIOPHYSICAL ECOLOGY OF LEAF MINERS

The biophysical functioning of a mine (i.e. the interplay between physical properties of a mine and abiotic factors) is based on the modifications provided by a larva to the absorbance properties of the mine surface and to the stomatal responses to changes in environmental conditions (Pincebourde & Casas 2006a,b; Pincebourde *et al*. 2006). Larvae induce an increase in the absorbance of near infrared radiation by creating feeding windows. Also, stomata below a mine are closing as radiation level is increasing, whereas they are opening in an intact leaf. The interaction between mine properties and radiation level explains why the temperature difference between shaded and sunny mines was higher during sunny conditions than during cloudy days. The biophysical properties of the mine allow the sunny mine temperature to rise much more than sunny leaf temperature do. These characteristics would, however, be risky during hot conditions without any feedback mechanism in the mine temperature regulation. Indeed, mines have the ability to control partly for overheating (Pincebourde & Casas 2006a). Without such a mechanism, body temperatures of larvae within sunny mines would be expected to be well above 42 °C during hot days. Modulation of heat stress through the manipulation of the biotic environment has been shown in other sedentary organisms such as mussels (Helmuth 1998). Interestingly, organisms living sometimes near their thermal limits such as leaf miners, mussels (Helmuth 1998) and *Drosophila* (Feder, Blair & Figueras 1997a,b) are showing original mechanisms to decrease their body temperature by only a few degrees. This might be sufficient to increase survival during extreme thermal events by a large margin.

THE CANOPY MOSAIC OF HERBIVORE MICROHABITATS IS DYNAMIC

Variations in regional climatic parameters induce the mosaic of microhabitats to be dynamic. We clearly observed that the thermal heterogeneity in mine microclimates at canopy scale substantially differed between cloudy and sunny conditions. The impact was only quantitative during moderate conditions and no shift in habitat suitability is expected as long as the temperatures are still between the minimum required for the development and the optimal temperature. Within this temperature range, sunny mines are likely to be always the more favourable microhabitat for the insect development. Based on these observations, we however expect that conditions within sunny mines would become risky for insect survival during extreme temperature event. The model exploration provided us with both qualitative and quantitative mechanistic details.

The developmental rate of fifth stage *P. blancardella* larvae is maximal at body temperatures between 35 °C and 38 °C. Body temperatures predicted within sunny mines at midday during the warm day match this optimal body temperature range while that predicted for shaded mines was never above 30 °C. The differences in microclimate between sunny and shaded locations within the canopy caused the instantaneous developmental rate inside sunny mines to be substantially faster than that within shaded mines at midday during a warm day. Conversely, body temperature of larvae within sunny mines falls within the range of thermal stress for several hours during the hot day. The instantaneous developmental rate was therefore considerably lowered. Indeed, the slope of the developmental rate curve is so steep between body temperature 38 °C and 42 °C that even a slight increase of about 1·5 °C leads to a large decrease of about 48% in the developmental rate. This explains why large standard deviations were obtained in the mean instantaneous developmental rate of larvae within sunny mines during the hot day (Fig. 11).

The canopy geometry both magnifies and reduces the heterogeneity of microclimatic conditions experienced by an insect, compared with the regional conditions. The high temperatures occurring during heat waves induce a reversal between the best and worst locations for development. The sunny location is optimal for larval development under warm climatic conditions, but becomes risky for survival under hot conditions. By contrast, shaded locations are suboptimal for larval development under moderate and warm climatic conditions and optimal during hot summers. It should be noted, however, that microclimate quality is not the only parameter of importance for herbivores living within tree canopies.

SHIFTING MOSAIC AND INSECT DISTRIBUTIONS

Orians & Jones (2001) qualified plants canopies as resource mosaics and sorted out the numerous abiotic and biotic factors causing this heterogeneity. Leaf nutritional quality varies, among others, as a function of light environment, temperature and soil nutrients (e.g. Lawler *et al*. 1997; Le Corff & Marquis 1999). Moreover, predators and parasitoids might not forage uniformly within tree canopies. For example, herbivores can be less exposed to predators when resting on leaves inside canopies compared with leaves at the periphery where they are more visible (e.g. Tschanz, Schmid &

Bacher 2005). The foraging behaviour of parasitoids can also depend on the level of heterogeneity in herbivore density within the canopy (e.g. Casas 1990; Casas & Djemai 2002). It is not known whether the canopy-scale mosaics of leaf nutritional quality and predation pressure are dynamic, and if so over which temporal windows, and whether their heterogeneity can be modified by variations in climatic conditions.

Thus, the relative importance of microclimatic conditions in the mother's decision for oviposition sites cannot be fully assessed yet. Leaf miners are sessile organisms and the microhabitat characteristics of a larva clearly depends on the oviposition site previously chosen by the female. It is not known whether females of leaf mining insects are able to discriminate between leaves that will provide the optimal microclimate to larvae and those that will not, but that seems to be a difficult task. For example, adult and larva of *Drosophila melanogaster*, which is feeding on necrotic fruits, also have behaviours that can potentially exploit the environmental heterogeneity to avoid thermally lethal conditions (Feder *et al*. 1997a). But even so, larvae still undergo stressful and often lethal conditions in the field (Feder *et al*. 1997b). No stratification in *P. blancardella* larvae density was found within apple tree canopies, and the distribution seems rather uniform over height (Pottinger & LeRoux 1971; Casas 1990). In other leaf mining species, when a density gradient has been measured, it was shown to be caused by biotic factors rather than by climatic parameters (e.g. Brown *et al*. 1997). Indeed, the distribution of leaf mining larvae within tree canopies probably reflects a trade-off between several concurrent pressures. A uniform distribution might be the best one to choose when the number of influencing factors is so large and the mosaic of favourable and risky habitats so dynamic.

The canopy geometry induces a large heterogeneity of microclimatic conditions for the leaf miner. Favourable and risky spots within the canopy do change as function of the climatic conditions at the regional scale. Extreme climatic events lead to deadly risks of overheating at specific locations otherwise optimal for the leaf miner's growth. The reversal of suitability of microhabitats as a function of extreme climatic conditions is striking and may well apply to many other biological systems for which such detailed and comprehensive models are not available. This climate-induced dynamic of the microhabitat heterogeneity within canopies could lead to strong modifications in the population dynamics of herbivores through differential mortality. Ultimately, our approach can be used to determine under which conditions climate variations lead to mere local change in microhabitat use and under which conditions more severe shifts in geographical distribution are mandatory.

Acknowledgements

The authors are grateful to Jean Guern and Dominique Lidoreau for giving us access to the apple tree. We acknowledge Brian Helmuth for his comments on the manuscript. This study was mainly funded by a PhD scholarship from the French Ministry for Education and Research to S.P. and by the ACI 'Ecologie Quantitative' project 'Ecologie Physique' led by J.C.

References

Ackerly, D.D. & Bazzaz, F.A. (1995) Seedling crown orientation and interception of diffuse radiation in tropical forest gaps. *Ecology*, **76**, 1134–1146.

Adam, B. (1999) *POL95-Software to Drive a Polhemus Fastrak 3 SPACE 3D Digitiser*, *Version* 1·0. UMR PIAF INRA-UBP, Clermont-Ferrand.

Adam, B., Sinoquet, H. & Donès, N. (2001) *Vegestar – Software to Compute Light Interception and Canopy Photosynthesis from Images of 3D Digitised Plants*, Version 2·0. UMR PIAF INRA-UBP, Clermont-Ferrand.

Baumgartner, J., Delucchi, V. & Genini, M. (1981) Taxonomic characters and physiological responses to temperature and photoperiod of two Lithocolletis species mining apple leaves. *Bulletin de la Société Entomologique Suisse*, **54**, 245–255.

Baumgartner, J. & Severini, M. (1987) Microclimate and arthropod phenologies: the leaf miner *Phyllonorycter blancardella* F. (Lep) as an example. *International Conference on Agrometeorology* (eds F. Prodi, F. Rossi & F. Cristoferi), pp. 225–243. Fondazione Cesena Agricultura Publications, Cesena., Italy.

Brown, J.L., Vargo, S., Connor, E.F. & Nuckols, M.S. (1997) Causes of vertical stratification in the density of *Cameraria hamadryadella*. *Ecological Entomology*, **22**, 16–25.

Campbell, G.S. & Norman, J.M. (1998) *Plants and Plant Communities*. Springer Verlag, New York.

Casas, J. (1990) Multidimensional host distribution and nonrandom parasitism: a case study and a stochastic model. *Ecology*, **71**, 1893–1903.

Casas, J. & Djemai, I. (2002) Plant canopy architecture and multitrophic interactions. *Multitrophic Interactions* (eds T. Tscharnke & B. Hawkins), pp. 174–196. Cambridge University Press, Cambridge.

Casey, T.M. (1992) Biophysical ecology and heat exchange in insects. *American Zoologist*, **32**, 225–237.

Chown, S. & Nicolson, S. (2004) *Insect Physiological Ecology: Mechanisms and Patterns*. Oxford University Press, Oxford.

Combes, D., Sinoquet, H. & Varlet-Grancher, C. (2000) Preliminary measurement and simulation of the spatial distribution of the morphogenetically active radiation (MAR) within an isolated tree canopy. *Annals of Forest Science*, **57**, 497–511.

Costes, E., Sinoquet, H., Kelner, J.J. & Godin, C. (2003) Exploring within-tree architectural development of two apple tree cultivars over 6 years. *Annals of Botany*, **91**, 91–104.

Coxwell, C.C. & Bock, C.E. (1995) Spatial variation in diurnal surface temperatures and the distribution and abundance of an alpine grasshopper. *Oecologia*, **104**, 433–439.

Daudet, F.A., Le Roux, X., Sinoquet, H. & Adam, B. (1999) Wind speed and leaf boundary layer conductance variation within tree crown: consequences on leaf-to-atmosphere coupling and tree functions. *Agricultural and Forest Meteorology*, **97**, 171–185.

Djemai, I., Meyhöfer, R. & Casas, J. (2000) Geometrical games between a host and a parasitoid. *American Naturalist*, **156**, 257–265.

Durand, J.B., Guédon, Y., Caraglio, Y. & Costes, E. (2005) Analysis of the plant architecture via tree-structured statistical models: the hidden Markov tree models. *New Phytologist*, **166**, 813–825.

Easterling, D.R., Meehl, G.A., Parmesan, C., Changnon, S.A., Karl, T.R. & Mearns, L.O. (2000) Climate extremes: observations, modeling, and impacts. *Science*, **289**, 2068–2074.

Feder, M.E., Blair, N. & Figueras, H. (1997a) Oviposition site selection: unresponsiveness of *Drosophila* to cues of potential thermal stress. *Animal Behaviour*, **53**, 585–588.

Feder, M.E., Blair, N. & Figueras, H. (1997b) Natural thermal stress and heat-shock protein expression in *Drosophila* larvae and pupae. *Functional Ecology*, **11**, 90–100.

Gates, D.M. (1980) *Biophysical Ecology*. Springer-Verlag, New York.

Gilman, S.E., Wethey, D.S. & Helmuth, B. (2006) Variation in the sensitivity of organismal body temperature to climate change over local and geographic scales. *Proceedings of the National Academy of Sciences USA*, **103**, 9560–9565.

Grace, J. (1991) Physical and ecological evaluation of heterogeneity. *Functional Ecology*, **5**, 192–201.

Helmuth, B.S.T. (1998) Interdidal mussel microclimates: predicting the body temperature of a sessile invertebrate. *Ecological Monographs*, **68**, 51–74.

Helmuth, B. (2002) How do we measure the environment? Linking intertidal thermal physiology and ecology through biophysics. *Integrative and Comparative Biology*, **42**, 837–845.

Helmuth, B., Kingsolver, J.G. & Carrington, E. (2005) Biophysics, physiological ecology, and climate change: Does mechanism matter? *Annual Review of Physiology*, **67**, 177–201.

Huey, R.B., Peterson, C.R., Arnold, S.J. & Porter, W.P. (1989) Hot rocks and not-so-hot rocks: retreat-site selection by garter snakes and its thermal consequences. *Ecology*, **70**, 931–944.

Impens, I. & Lemeur, R. (1969) Extinction of net radiation in different crop canopies. *Theoretical and Applied Climatology*, **17**, 403–412.

Kitajima, K., Mulkey, S.S. & Wright, S.J. (2005) Variation in crown light utilization characteristics among tropical canopy trees. *Annals of Botany*, **95**, 535–547.

Lawler, L.R., Foley, W.J., Woodrow, I.E. & Cork, S.J. (1997) The effects of elevated CO_2 atmospheres on the nutritional quality of Eucalyptus foliage and its interaction with soil nutrient and light availability. *Oecologia*, **109**, 59–68.

Le Corff, J. & Marquis, R.J. (1999) Differences between understorey and canopy in herbivore community composition and leaf quality for two oak species in Missouri. *Ecological Entomology*, **24**, 46–58.

Logan, J.A., Wollkind, D.J., Hoyt, S.C. & Tanigoshi, L.K. (1976) An analytic model for description of temperature dependent rate phenomena in arthropods. *Environmental Entomology*, **5**, 1133–1140.

Montgomery, R.A. & Chazdon, R.L. (2001) Forest structure, canopy architecture, and light transmittance in tropical wet forests. *Ecology*, **82**, 2707–2718.

Nobel, P.S. (1999) *Physicochemical and Environmental Plant Physiology*, 2nd edn. Academic Press, New York.

Nougier, J.P. (1985) *Méthodes de Calcul Numérique*. 2nd edn. Masson, Paris.

Orians, C.M. & Jones, C.G. (2001) Plants as resource mosaics: a functional model for predicting patterns of within-plant resource heterogeneity to consumers based on vascular architecture and local environmental variability. *Oikos*, **94**, 493–504.

Pincebourde, S. (2005) *Biophysique environnementale des insectes endophytes*. PhD Thesis, University François Rabelais, Tours, France.

Pincebourde, S. & Casas, J. (2006a) Multitrophic biophysical budgets: thermal ecology of an intimate herbivore insect–plant interaction. *Ecological Monographs*, **76**, 175–194.

Pincebourde, S. & Casas, J. (2006b) Leaf miner-induced changes in leaf transmittance cause variations in insect respiration rates. *Journal of Insect Physiology*, **52**, 194–201.

Pincebourde, S., Frak, E., Sinoquet, H., Regnard, J.L. & Casas, J. (2006) Herbivory mitigation through increased water use efficiency in a leaf mining moth-apple tree relationship. *Plant, Cell and Environment*, **29**, 2238–2247.

Porter, W.P. & Gates, D.M. (1969) Thermodynamic equilibria of animals with environment. *Ecological Monographs*, **39**, 245–270.

Pottinger, R.P. & LeRoux, E.J. (1971) The biology and the dynamics of *Lithocolletis blancardella* (Lepidoptera: Gracillariidae) on apple in Quebec. *Memoirs of the Entomological Society of Canada*, **77**, 1–437.

Seneviratne, S.I., Luthi, D., Litschi, M. & Schar, C. (2006) Land-atmosphere coupling and climate change in Europe. *Nature*, **443**, 205–209.

Sinoquet, H. & Bonhomme, R. (1992) Modeling radiative transfer in mixed and row intercropping systems. *Agricultural and Forest Meteorology*, **62**, 219–240.

Sinoquet, H., Le Roux, X., Adam, B., Amaglio, T. & Daudet, F.A. (2001) RATP: a model for simulating the spatial distribution of radiation absorption, transpiration and photosynthesis within canopies: application to an isolated tree crown. *Plant, Cell and Environment*, **24**, 395–406.

Sinoquet, H., Thanisawanyangkura, S., Mabrouk, H. & Kasemsap, P. (1998) Characterization of the light environment in canopies using 3D digitising and image processing. *Annals of Botany*, **82**, 203–212.

Tschanz, B., Schmid, E. & Bacher, S. (2005) Host plant exposure determines larval vulnerability – do prey females know? *Functional Ecology*, **19**, 391–395.

Varlet-Grancher, C. (1975) Variation et estimation de l'énergie d'origine solaire reçue sur des plans d'inclinaison et d'azimut variables. *Annales Agronomiques*, **26**, 245–264.

Weiss, S.B., Murphy, D.D., Ehrlich, P.R. & Metzler, C.F. (1993) Adult emergence phenology in checkerspot butterflies: the effects of macroclimate, topoclimate, and population history. *Oecologia*, **96**, 261–270.

Zar, J.H. (1998) *Biostatistical Analysis*. 4th ednn. Prentice Hall, New Jersey.

Received 17 October 2006; accepted 6 February 2007

Supplementary material

The following supplementary material is available for this article.

Appendix S1. Equations of the biophysical models.

This material is available as part of the online article from: http://www.blackwell-synergy.com/doi/full/10.1111/j.1365-2656.2007.01231.x.

Please note: Blackwell Publishing is not responsible for the content or functionality of any supplementary materials supplied by the authors. Any queries (other than missing material) should be directed to the corresponding author for the article.

REGIONAL CLIMATE MODULATES THE CANOPY MOSAIC OF FAVOURABLE AND RISKY MICROCLIMATES FOR INSECTS

S. Pincebourde, H. Sinoquet, D. Combes & J. Casas

APPENDIX S1 – EQUATIONS OF THE BIOPHYSICAL MODELS

MODELLING RADIATION INTERCEPTION BY A CANOPY

The RATP model (Radiation Absorption, Transpiration and Photosynthesis) was designed to describe the spatial distribution of radiation, transpiration and photosynthesis within plant canopies. The full model is described in Sinoquet *et al.* (2001). Here, the sub-model simulating the interception of solar radiation by leaves at the intracanopy scale was used. The model is based on the Beer's law, the canopy being treated as a turbid medium. Inputs for this model are the canopy geometry, optical properties of leaves and soil surface and the climatic driving variables. The canopy geometry is described by discretising the space into a grid of 3D cubic cells (voxels). Each cell might be empty or characterized by the area density of a given plant component, according to 3D digitizing data. Here, one canopy component was defined, the leaves.

The radiative transfer sub-model is aimed at (i) sending beams into the canopy according to the directional distribution of incident radiation, by taking into account for the sun direction and the distribution of incident radiation into direct and diffuse radiation; radiance distribution for diffuse radiation is assumed to obey the standard overcast sky (SOC, Moon & Spencer 1942); (ii) identifying the 3D sequence of cells crossed by any light beam; (iii) determining the beam path length within each crossed cell; and (iv) applying Beer's law to calculate beam extinction within each crossed cell (Sinoquet *et al.* 2001). Radiation sources are the sky,

including direct and diffuse (i.e. scattered by clouds and atmospheric gases) fraction of incident radiation, as well as foliage components and soil surface which scatter a fraction of radiation they intercept. The flux of radiation (W/m^2) intercepted by a leaf, in cell *k*, in sunlit and shaded area is respectively

$$I_k^{sun} = I_k^{dc} + I_k^{df} + I_k^{L-sc} + I_k^{S-sc} \quad (1)$$

$$I_k^{shade} = I_k^{df} + I_k^{L-sc} + I_k^{S-sc} \quad (2)$$

where I_k^{dc} is the flux of direct radiation intercepted by a leaf in cell *k*, I_k^{df} is the intercepted flux of diffuse radiation, I_k^{L-sc} is the intercepted flux of radiation scattered by neighbouring leaves, and I_k^{S-sc} is the intercepted flux of radiation scattered by soil surface (all in W/m^2). The terms in equations (1) and (2) are detailed below.

The direct beam light is intercepted only by the sunlit leaf area. The flux of direct solar radiation intercepted by a leaf in cell *k* depends on the direction of the beam light (Ω) and is calculated from

$$I_k^{dc} = I_{bo} \frac{G_k(\Omega)}{\sin(h_{sun})} \quad (3)$$

where I_{bo} is the flux of direct radiation on a horizontal plane, h_{sun} is sun elevation, and $G_k(\Omega)$ is the projection of leaf area in cell *k* onto a plane perpendicular to beam light direction (Ω) and depends on inclination angle distribution of leaves within the cell *k*.

The flux of diffuse radiation intercepted by a leaf in cell *k* is

$$I_k^{df} = I_{do}\, C_{do \to k} \quad (4)$$

where I_{do} is the flux of incident diffuse radiation on a horizontal plane. $C_{do \to k}$ is the radiation exchange coefficient between the sky, which emits diffuse radiation, and leaves in cell *k*. The computation used to derived radiation exchange coefficients is given in Sinoquet *et al.* (2001).

The flux of radiation scattered by leaves in each grid cell and intercepted by a leaf in cell *k* is computed from

$$I_k^{L-sc} = \sum_{k'=1}^{K} I_{k'} \, \rho_L \, C_{k' \to k} \tag{5}$$

where $I_{k'}$ is the flux of radiation intercepted by leaves in cell *k'* (there are *K* cells), ρ_L is the scattering coefficient of leaves (obtained by summing transmittance and reflectance of leaves), and $C_{k' \to k}$ is the radiation exchange coefficient between leaves in cell *k'* and those in cell *k*.

The flux of radiations scattered by a soil unit surface *s* (there are *S* soil unit surfaces) and intercepted by leaves in cell *k* is determined by

$$I_k^{S-sc} = \sum_{s=1}^{S} I_s \, \rho_s \, C_{s \to k} \tag{6}$$

where I_s is the flux of radiation intercepted by the soil, ρ_s is the scattering coefficient of the soil, and $C_{s \to k}$ is the coefficient of radiation exchange from soil to leaves in cell *k*.

This model for interception of solar radiation was computed for both photosynthetically active radiation (PAR, 400 to 700 nm waveband) and near infrared radiation (NIR, 700 to 2500 nm waveband). Outputs are fluxes of PAR and NIR intercepted by both sunlit and shaded areas in each 3D cell occupied by leaves.

We used published biophysical models to compute the energy balance of leaves and mines (Campbell & Norman 1998; Nobel 1999; Pincebourde & Casas 2006a). The energy budget model of component *j* (a leaf or a mine) in cell *k* is

$$A_{jk}\left(Rn_{jk}+E_{jk}+H_{jk}\right)=0 \tag{7}$$

A_{jk} is the amount of surface of component *j* in cell *k*. Rn_j is the net radiation budget of the component *j*, E_j is the latent heat budget (i.e. heat lost during evaporation), and H_j is the sensible heat budget (i.e. heat lost during conduction and convection mechanisms) (all in W/m^2). Values of each term between brackets are positive or negative depending on the direction of the heat flux - gain or lost by the component, respectively. Energy storage by leaves and mines was neglected (Nobel 1999; Pincebourde & Casas 2006a). The terms of the energy budget are detailed below and are given for sunlit area only, as the equations also apply to compute energy budget in shaded area using parameters for shaded components.

The net radiation balance of component *j* in cell *k* is the sum of the radiative heat fluxes occurring in three wavebands, i.e. PAR, NIR and thermal infrared radiations (TIR), that is

$$Rn_{jk}^{sun}=a_j^{PAR}I_k^{sun,PAR}+a_j^{NIR}I_k^{sun,NIR}+a_j^{TIR}I_k^{sun,TIR}-2\varepsilon_j\,\sigma\,T_{jk}^{sun^4} \tag{8}$$

a_j^{PAR}, a_j^{NIR}, and a_j^{TIR} are absorbance of component *j* in each waveband. According to Kirchhoff's law, leaf absorbance in the TIR waveband equals emissivity, i.e. $a_j^{TIR}=\varepsilon_j=0.97$ (Campbell & Norman 1998). Fluxes $I_k^{sun,PAR}$ and $I_k^{sun,NIR}$ are computed from equation (1). The flux $I_k^{sun,TIR}$ is calculated from equation (1) assuming scattering coefficients of soil and component surfaces in TIR waveband are zero (Campbell & Norman 1998), and including the emitted TIR by neighbouring leaves (in sunlit and shaded areas as well) and soil unit surfaces (see Sinoquet *et al.* 2001). The last term on the right of equation (8) corresponds to TIR

emitted by component *j* in cell *k*. The amount of emitted TIR depends on the Stephan-Boltzman constant (σ = 5.67 10^{-8} W m^{-2} K^{-4}) and on temperature T_j of the component.

Each component *j* (leaves or mines) loses water vapour through lower and upper surfaces. The latent heat lost during evaporation is

$$E_{jk} = \lambda \, g_{jv}^{sun} \left(\frac{e_s\left(T_{jk}^{sun}\right) - e_a}{p_a} \right) \tag{9}$$

where λ is the latent heat of vaporization for water (λ = 44 kJ/mol at 25°C), g_{jv}^{sun} is the conductance for water vapour transfer of component *j* (mol m^{-2} s^{-1}), $e_s\left(T_{jk}^{sun}\right)$ is the saturated water vapour pressure (Pa) at temperature T_{jk}^{sun} (°C) of the component *j* in cell *k*, e_a is the water vapour pressure in the air (Pa) and p_a is the atmospheric pressure (101.3 x 10^3 Pa). Water vapour pressure in the air was assumed to be constant within the tree canopy, as confirmed by Daudet *et al.* (1999). In hypostomatous leaves, the conductance for water vapour transfer is calculated by combining conductance of the boundary layer (g_{jva}^{sun}) and conductance through upper (transpiration through epidermis) and lower (through stomata) sides of component *j* ($g_{jk}^{u,sun}$ and $g_{jk}^{st,sun}$ respectively), that is

$$g_{jv}^{sun} = \frac{0.5}{\frac{1}{g_{jva}^{sun}} + \frac{1}{g_{jk}^{u,sun}}} + \frac{0.5}{\frac{1}{g_{jva}^{sun}} + \frac{1}{g_{jk}^{st,sun}}} \tag{10}$$

We used the model of Jarvis (1976) according to which the effect of each climatic variable on stomatal conductance is independent from each over (non-synergetic interactions). Stomatal conductance was therefore calculated by

$$g_{jk}^{st,sun} = g_j^{\max} \; f_j^1\left(I_{jk}^{sun,PAR}\right) \, f_j^2\left(e_s\left(T_{jk}^{sun}\right) - e_a\right) \, f_j^3\left(T_{jk}^{sun}\right) \tag{11}$$

where $g_j^{\max}$ is the maximal stomatal conductance (mol m^{-2} s^{-1}), attained under specific levels of irradiance ($I_{jk}^{sun,PAR}$: µmol PAR m^{-2} s^{-1}), water vapour pressure deficit of component *j*

($\left(e_s\left(T_{jk}^{sun}\right)-e_a\right)$: Pa) and component's temperature (T_{jk}^{sun}: °C), and f_j^1, f_j^2, and f_j^3 are the functions describing the variations of the stomatal conductance relative to the maximal value following a change in irradiance level, water vapour pressure deficit and component temperature, respectively.

The sensible heat budget of sunlit leaves (subscript *L*) in cell *k* is given by

$$H_{Lk} = c_p\ g_L^{ha}\left(T_{Lk}^{sun} - T_{air}\right) \tag{12}$$

where c_p is the specific heat of the air (29.3 J mol^{-1} °C^{-1}), and T_{air} is air temperature (K). Air temperature was assumed to be constant within the tree canopy. The leaf boundary layer conductance for heat under forced convection mechanisms (g_L^{ha}: mol m^{-2} s^{-1}) was computed from local wind speed (i.e. wind speed at a leaf surface) using the method given in Pincebourde & Casas (2006a). Local wind speed was obtained from wind speed values taken above the canopy using the empirical relationships between wind speed attenuation and the total amount of foliage along wind vector given in Daudet *et al.* (1999).

The sensible heat budget of sunlit mines (subscript *M*) in cell *k* is calculated by

$$H_{Mk} = c_p\ g_M^{ha}\left(T_{Mk}^{sun} - T_{air}\right) + \frac{P_M}{S_M}\, c_p\ g_M^{hl}\left(T_{Mk}^{sun} - T_{Lk}^{sun}\right) \tag{13}$$

where g_M^{ha} is the mine boundary layer conductance for heat under forced convection process ($g_M^{ha} = g_L^{ha}$, Pincebourde & Casas 2006a). The second term on the right in equation (13) computes the amount of heat exchanged between a mine and its leaf through convection mechanism. This term needs to be transformed to be expressed in the same unit surface as the first term in the equation. This is achieved by computing the leaf-mine interface area (P_M) relative to the mine upper area (S_M). The conductance for heat in the leaf-mine contact area (g_M^{hl}) occurs under free convection assumption (Pincebourde & Casas 2006a).

The energy balance (equation (7)) was solved for temperature using the iterative Newton-Raphson method (Nougier 1985). Outputs of the energy budget model are temperatures of both leaves and mines in sunlit and shaded areas within each 3D cell of the canopy (T_{Lk}^{sun}, T_{Mk}^{sun}, T_{Lk}^{shade} and T_{Mk}^{shade}).

REFERENCES

Campbell, G.S. & Norman, J.M. (1998) Plants and plant communities. *An Introduction to Environmental Biophysics* (eds G.S. Campbell & J.M. Norman), pp. 223-246. Springer Verlag, New York.

Daudet, F.A., Le Roux, X., Sinoquet, H., & Adam, B. (1999) Wind speed and leaf boundary layer conductance variation within tree crown: consequences on leaf-to-atmosphere coupling and tree functions. *Agricultural and Forest Meteorology*, **97**, 171-185.

Jarvis, P.G. (1976) The interpretation of the variations in leaf water potential and stomatal conductance found in canopies in the field. *Philosophical Transactions of the Royal Society of London Series B*, **273**, 593-610.

Moon, P. & Spencer, D.E. (1942) Illumination from a non-uniform sky. *Transactions of the Illumination Engineering Society*, **37**, 707-712.

Nobel, P.S. (1999) *Physicochemical & Environmental Plant Physiology*, Second edn. Academic Press, New York.

Nougier, J.P. (1958) *Méthodes de calcul numérique*, Second edn. Masson, Paris.

Pincebourde, S. & Casas, J. (2006a) Multitrophic biophysical budgets: thermal ecology of an intimate herbivore insect-plant interaction. *Ecological Monographs*, **76**, 175-194.

Sinoquet, H., Le Roux, X., Adam, B., Amaglio, T., & Daudet, F.A. (2001) RATP: a model for simulating the spatial distribution of radiation absorption, transpiration and photosynthesis within canopies: application to an isolated tree crown. *Plant, Cell and Environment*, **24**, 395-406.